Quasicritical coupling in a few-mode tapered-fiber coupled whispering-gallery-mode system

Xiaoting Li,[1] Pengfa Chang,[1] Ligang Huang,[2] Feng Gao,[1,*] Wending Zhang,[3] Fang Bo,[1] Guoquan Zhang,[1] and Jingjun Xu[1,†]

[1]*MOE Key Laboratory of Weak-Light Nonlinear Photonics, TEDA Institute of Applied Physics and School of Physics, Nankai University, Tianjin 300457, China*

[2]*Key Laboratory of Optoelectronic Technology and Systems (Ministry of Education), Chongqing University, Chongqing 400044, China*

[3]*MOE Key Laboratory of Material Physics and Chemistry under Extraordinary Conditions and Shaanxi Key Laboratory of Optical Information Technology, School of Science, Northwestern Polytechnical University, Xi'an 710072, China*

(Received 21 June 2018; published 9 November 2018; corrected 3 December 2018)

A quasicritical coupling state was demonstrated both in theory and experiment with a few-mode tapered-fiber (TF) coupled whispering-gallery-mode (WGM) cavity. In such a configuration, the coupling mode to activate the WGM and the drop mode are in the same TF and of almost the same decay rate with the variation of the gap between the TF and WGM cavity. Consequently, when the gap decreases to zero, the transmission of the coupling mode decreases monotonously to zero at the resonance wavelength, while the transmission of the drop mode increases monotonously to unit, which means that neither the coupling efficiency in the coupling mode nor the transmission of the drop mode will decrease in the traditional overcoupling region. Thus a steadily high coupling efficiency can be achieved accordingly, which we defined as quasicritical coupling. Such a coupling state will be helpful to develop WGM-cavity-based filters and benefit the fabrication of ultranarrow-linewidth lasers.

DOI: 10.1103/PhysRevA.98.053814

I. INTRODUCTION

High-quality factor (Q-factor) optical whispering-gallery-mode (WGM) microresonators have attracted much attention because they can be widely used in quantum information, nonlinear optics, ultranarrow-linewidth lasers, and label-free sensors [1–5]. Most of their applications and studies are based on a simple coupling method utilizing a single-mode tapered fiber (TF) because it is not only simple, but also could attain almost 100% coupling efficiency under the condition of critical coupling [6]. However, a slight position deviation between the cavity and the TF would result in a deviation from the critical coupling to the undercoupling or overcoupling with a decreased coupling efficiency [6]. The nonmonotonously varied coupling efficiency easily causes bidirectional instability, and the situation is even worse when the configuration is applied in an add-drop filter, which could provide both band-pass and band-rejection spectra, typically with two single-mode TFs coupling to a microresonator at each side [7–9]. Note that such a structure was also applied in the research of spontaneous chirality in the WGM resonator for it could provide the same coupling rate for both clockwise and counterclockwise modes [10]. Stable add-drop efficiency demands high stability of both TFs and the microcavity. People have to develop various package methods for the TF-WGM system to make it more applicable [11,12], for example introducing an additional frame or just pasting TF with glue on the resonator. Before now, little attention has been paid to the coupling configuration itself.

Critical coupling in the cavity requires that the coupling loss to the TF is equal to its intrinsic loss [13]. The instability comes from the fact that such a coupling loss to the TF is sensitive to the relative position between the TF and the microcavity while the intrinsic loss of the cavity is not, which is determined by the cavity itself, such as the absorption of the material, the scattering of residual inhomogeneity, the curvature and roughness of the surface [14], etc. In our previous work, we demonstrated that the WGM cavity could realize mode conversion in a few-mode TF [15]. The cascaded mode conversions in a piece of few mode fiber based on the WGM microcavities could be further applied in the generation of in-fiber vector beams and an optical vortex [16,17]. With the LP_{11} mode acting as the drop mode, which actually played the role of an additional loss to the cavity, it may balance the losses and solve the problem mentioned above.

In this paper, we explore theoretically and experimentally the coupling state in a few-mode TF coupled microcavity system. With the TF supporting both LP_{01} and LP_{11} modes, the system could work in a quasicritical coupling state under certain conditions: more than 98% energy of the LP_{01} mode could be coupled to the cavity as the distance between the TF and the cavity decreased to zero. Compared to a single-mode TF, the quasicritical resonance coupling efficiency is monotonously varied with distance, and the contacting-coupling offers great stability and operability with almost 100% coupling efficiency for practical applications. More importantly, the resonance transmission of the drop mode (LP_{11}) can also be almost unit under the quasicritical coupling and inherit the same stability. The configuration provides additional stability to the coupling

*fenggao@nankai.edu.cn
†jjxu@nankai.edu.cn

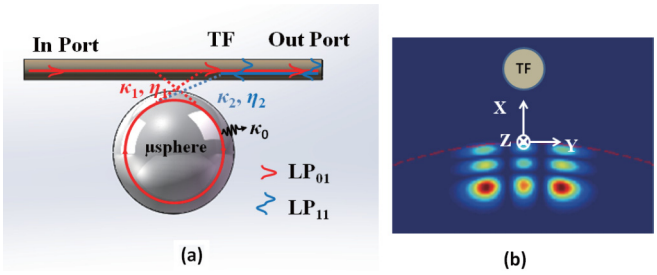

FIG. 1. (a) The coupling system of a few-mode TF and a microsphere. In the figure, the two modes of LP_{01} and LP_{11} are taken into consideration. (b) A typical mode of the microsphere as $TE_{3,549,547}$ and the coordinate used for calculation (right side view of the coupling system).

system with high add-drop efficiency and will bring more operability to its applications and research.

II. CONFIGURATION AND THEORY

We know that the instability of the coupling results from the imbalance between the coupling loss to the TF and the intrinsic loss of the cavity. With an additional loss that could compensate for the fluctuation of the coupling loss, the stability of the system could be improved. In a previous report, the critical coupling could be realized by introducing an additional loss from a second TF [9]. However, since the two TFs were independent, such a coupling state was still unstable. Therefore, to get a stable coupling state, the two losses have to be associated with each other. In this work, the problem is solved by coupling the WGM microcavity to a few-mode fiber with a second mode of the fiber acting as the additional loss. In a structure consisting of a WGM cavity and a two-mode TF, which supports both LP_{01} and LP_{11} modes as shown in Fig. 1(a), with the input light being the LP_{01} mode, the transmission of it could be given as [9]

$$T = \frac{A_2^2}{A_1^2} = \frac{4\delta\omega^2 + (\kappa_0 - \kappa_1 + \kappa_2)^2}{4\delta\omega^2 + (\kappa_0 + \kappa_1 + \kappa_2)^2}, \tag{1}$$

where κ_0, κ_1, and κ_2 are the cavity intensity decay rates due to the intrinsic loss, the coupling loss to the LP_{01} fiber mode, and the coupling loss to the LP_{11} fiber mode, respectively.

When $\delta\omega = 0$, $\kappa_1 >> \kappa_0$, and $\kappa_2 >> \kappa_0$, the transmission can be presented as

$$T = \frac{A_2^2}{A_1^2} = \frac{\left(1 - \frac{\kappa_1}{\kappa_2}\right)^2}{\left(1 + \frac{\kappa_1}{\kappa_2}\right)^2} = \frac{(1-\xi)^2}{(1+\xi)^2}, \tag{2}$$

where $\xi = \kappa_1/\kappa_2$. From Eq. (2), it is clear that the transmission will remain constant with ξ being a constant. In a high-Q cavity, κ_0 is usually very small, and the transmission could be described by Eq. (2). If κ_1 and κ_2 fluctuate at the same rate with their proportion being a constant, the coupling efficiency will remain stable. In particular, the coupling state with $\xi = 1$, i.e., $\kappa_1 = \kappa_2 >> \kappa_0$, is defined as quasicritical coupling.

Similarly, the drop efficiency to the LP_{11} mode will also remain stable according to the following relationship [9]:

$$D = \frac{A_3^2}{A_1^2} = \frac{\frac{4\kappa_1}{\kappa_2}}{\left(1 + \frac{\kappa_1}{\kappa_2}\right)^2} = \frac{4\xi}{(1+\xi)^2}. \tag{3}$$

In the quasicritical coupling state, it is obvious that $T = 0$ and $D = 1$, which can be applied in the fabrication of an ideal add-drop filter (ADF) based on a WGM cavity providing both band-pass and band-rejecting functions. The coupling coefficient is determined by the overlapping of the mode fields of the TF and microcavity at the resonance wavelength, and the coupling efficiency could be calculated to give us more details on the state of the quasicritical coupling. The coupling losses could be given as the following equations [18]:

$$\eta_{sf} = \eta_{fs}^* = \frac{\omega\Delta\varepsilon}{4} \iiint_{V_s} \vec{E}_f \cdot \vec{E}_s^* \exp(i\Delta\beta z) ds\, dz, \tag{4}$$

$$\eta = |\eta_{sf}|^2 = |\eta_{fs}|^2, \tag{5}$$

$$e^{-\kappa\tau} = 1 - \eta, \tag{6}$$

where η_{sf} is the coupling coefficient of a fiber-mode to a WGM, and η_{sf} is the coupling coefficient of the fiber-mode to the WGM accordingly; $\tau = 2\pi n_s r_s/c$ is the one-loop circulation time for the light traveling inside the microsphere, n_s is the effective refractive index of the microsphere WGM, r_s is the radius of the microsphere, and c is the light speed in vacuum; $\Delta\varepsilon$ denotes the permittivity difference between the microsphere and the air, and $\Delta\beta = \beta_f - \beta_s$ defines the difference in the propagation constants of the fiber mode and WGM; $\vec{E}_f$ and $\vec{E}_s^*$ are the normalized fields of the fiber mode and the WGM, which are defined by $1/2 \iint \sqrt{\varepsilon/\mu_0} |\vec{E}_{f(s)}|^2 dx\, dy = 1$, and V_s is the volume of the microsphere. Typically, the origin of the coordinate is selected on the surface of the sphere, x refers to the distance between the TF and the microsphere, and the WGM of the microsphere is an even function in the Y direction, as shown in Fig. 1(b). η is defined as the ratio of power coupled between the fiber mode and WGM per revolution when light propagates in the microresonator.

Based on Eqs. (4), (5), and (6), it is convenient for us to give the simulation result of κ [19]. Allowing for the diameter of the TF being almost uniform, in which the fiber mode field distribution is almost unchanged along the Z axis, it is obvious that the displacement along Z will not change the coupling efficiency. There are various modes possible in a microcavity, especially in a microsphere. We select a typical mode $TE_{3,549,547}$ in a microsphere as an example to show the calculation result, which has an effective refractive index (ERI) between those of the LP_{01} and LP_{11} fiber modes to enable the two fiber modes to couple the microsphere simultaneously [14]. The diameter of the microsphere is 250 μm, whose traverse mode field and the coordinate used are shown in Fig. 1(b).

Figure 2 provides the typical calculation results of κ, ξ, and the coupling efficiency when the microsphere's position varies along the X and Y axes accordingly. In Figs. 2(a1) and 2(a2), κ_1, κ_2, and κ_0 are presented as a red dashed curve, a blue dash-dotted curve, and a pink dotted curve, respectively. The variation of ξ in each direction is given in Figs. 2(b1) and

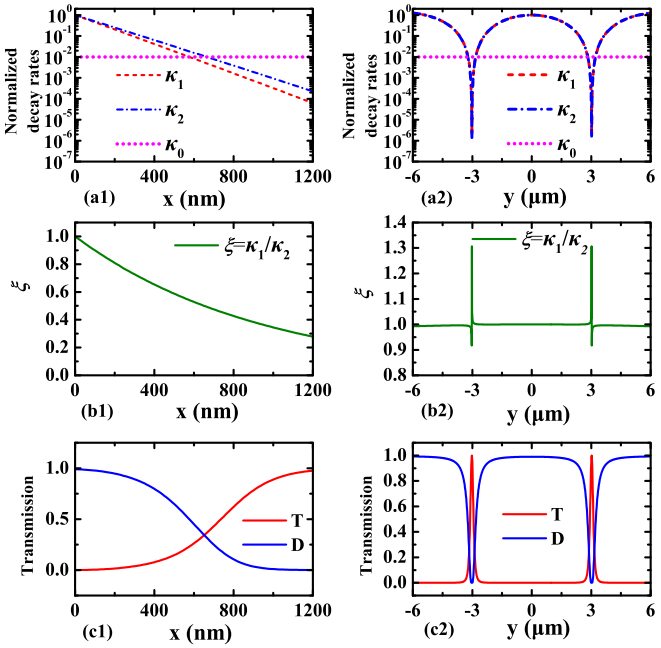

FIG. 2. The calculated results of normalized decay rates, ξ, and coupling efficiencies in the X and Y directions. The calculation is based on the coupling between $TE_{3,549,547}$ in a microsphere as shown in Fig. 1(b) and a few-mode TF. Parts (a1) and (a2) are the normalized decay rates with the typical intrinsic loss κ_0 set to be much smaller than the coupling damping rates at the origin of the coordinate; (b1) and (b2) are the results for ξ accordingly; (c1) and (c2) depict the coupling efficiencies of the drop port (D) and through port (T).

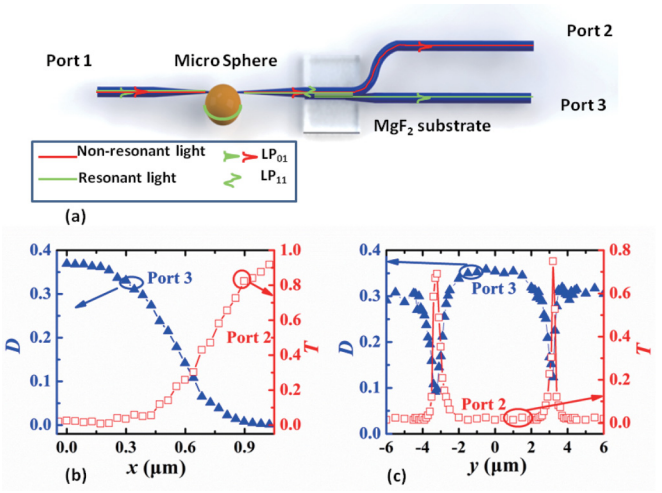

FIG. 3. The experimental configuration and its results of the coupling efficiencies in a few-mode TF-microsphere system. (a) The experimental configuration. The modes in red are at the nonresonant wavelength, while the modes in green are at the resonant wavelength of the WGM cavity; (b) and (c) are the measured coupling efficiencies when the gap and position between the few-mode TF and the microsphere were tuned in the X and Y directions, respectively. T and D in the theory denote the resonance transmissions of Port 2 (Through Port) and Port 3 (Drop Port), respectively. Note that the original point in X is manually selected: we assume that when the TF is attached to the cavity, i.e., $x = 0$, the bandwidth will not change as the TF moves further toward the cavity.

2(b2). The calculated coupling efficiency of each mode is also shown in Figs. 2(c1) and 2(c2). The through port is shown as the red solid curve, while the drop port is shown as the blue solid curve. It is clear that when the TF is approaching the microsphere, the drop efficiency is almost unit, which means that the critical coupling could still be achieved even though the coupling losses κ_1 and κ_2 are much bigger than the intrinsic loss κ_0. Obviously, the contacting coupling could bring a more stable coupling than the traditional coupling via a single-mode TF [6]: on the one hand, it is more stable with the gap variation between the TF and WGM; on the other hand, the closely fitting condition could be robust as a result of the attraction force between the surfaces of the TF and the WGM resonator, which is convenient for the further package. When ξ deviates from unit, the coupling efficiency changes accordingly. At the same time, it is worth noting that the drop efficiencies both decrease sharply in both the X and Y directions at a certain position where κ_1 and κ_2 are not much larger than κ_0, as shown in Figs. 2(a1) and 2(a2).

III. EXPERIMENTAL RESULTS

In the configuration with a few-mode TF and a microsphere as shown in Fig. 3(a), we measured the through and drop transmissions of the structure as we changed the relative position between the microsphere and the TF in the X and Y directions, which was precisely controlled by a 3D nanopositioning system. The modes in green are at the resonant wavelength of the microsphere, while the modes in red are not. Note an additional TF was applied in the configuration to get the drop mode, which was actually the ADF structure as we reported previously [15].

In the experiment, the silica microsphere was fabricated with a diameter of 240 μm. A tunable laser with the central wavelength around 1550 nm was used to test the ADF structure. The diameter of the tapered fiber waist was prepared to be around 2.5 μm by the heat-and-pull method over a hydrogen flame. The tapered fiber had a transition zone of about 20 mm, which was long enough to keep quite a small taper angle in order to satisfy the adiabatic propagation condition for both LP_{01} and LP_{11} modes [20]. The microsphere was placed on a 3D nanopositioning system to precisely tune the position relative to the tapered fiber. To lead out the LP_{11} as the drop port, the same setup as our previous work was used [15,21]. The pigtail of the tapered fiber was etched to a diameter of 30 μm with hydrofluoric acid to increase the evanescent wave of the LP_{11} mode, and another tapered fiber with a diameter of 18 μm and its waist length of 15 mm was placed parallel to the etched fiber in order to lead the LP_{11} mode out. The coupling region between the two parallel fibers was dipped into refractive-index matched liquid ($n = 1.40$) to increase the coupling efficiency, and the coupling region was supported by a piece of MgF_2 substrate with a lower refractive index of ~1.37.

Before the measurement, the transmission of the through port at the resonant wavelength around 1550.670 nm was optimized to be almost zero by moving the microsphere along the TF (Z axis) as in our previous work [15] when the TF

was attached to the microsphere, i.e., $x = 0$. After that, the gap was tuned larger than zero by tuning the nanostage along the X direction, and then the transmission spectra of the resonant wavelength at the through port and the drop port were measured, when the position between the TF and the microsphere was tuned in the X and Y directions, respectively. In the measurement along the X direction, the TF was tuned to approach the microsphere. In the measurement along the Y direction, the TF was positioned with a minimum gap of around 50 nm to the microsphere and then swept from one side of the microsphere to the other. The achieved resonance transmissions of the through port (Port 2, denoted by T) and the drop port (Port 3, denoted by D) when the TF moved along the X and Y directions are presented in Figs. 3(b) and 3(c), respectively, which show good agreement with our calculated results, as shown in Figs. 2(c1) and 2(c2). Note that the coordinate origin in the X and Y directions in Figs. 3(b) and 3(c) is manually selected: when the TF is attached to the cavity, i.e., $x = 0$, the bandwidth will stop increasing obviously as the TF is further moving to the cavity. Because κ_1 and κ_2 would reach their maxima when x decreased to zero, the bandwidth was maximized considering the equation $\Delta\omega = \kappa_0 + \kappa_1 + \kappa_2$ [15]. The original point in Fig. 3(c) was selected to make the transmissions symmetric allowing for the WGM symmetry of the microsphere resonator. At the contacting-coupling point with $x = 0$, the quasicritical coupling was achieved with $T = 0.02$ and $D = 0.37$, which could remain nearly constant with the gap within 300 and 200 nm, respectively.

Note that in the X direction, the quasicoupling efficiency of the drop port when $x = 0$ was high enough considering the insertion loss around -3.5 dB (45%) of the parallel-waveguide evanescent wave coupling on the MgF_2 substrate [15]. In the Y direction, there is a region with flattened-profile high efficiency of the drop port. At the edge of this flattened area, the coupling efficiency drops quite fast within a very small distance. This happens when the microsphere mode number satisfies $l > m$, where l and m denote the polar mode number and the azimuthal mode number, respectively [19], and the TF lies at the node between two neighbored field maxima. Due to the high stability in the other directions (X and Z), this sharply changed efficiency could also be utilized in the nanoprecision position sensing along the Y axis.

IV. CONCLUSION

In conclusion, we demonstrated that a few-mode TF could realize the quasicritical coupling to a WGM cavity, which can achieve a 100% coupling efficiency when contacting the TF with the cavity. The coupling efficiency variation is monotonous to the distance between the TF and the microcavity. All of the features will benefit the structure as an application of a narrow band-reject filter. Moreover, the transmission of the drop mode (LP_{11}) can also be almost unit under the quasicritical coupling and inherited the same stability. With the drop mode led out, the add-drop filter, including both the band-pass filter and the band-reject filter, could be more stable based on such a configuration. The quasicritical coupling will benefit the fabrication of WGM-based add-drop filters, all-fiber ultranarrow-linewidth lasers, and high-precision sensors.

ACKNOWLEDGMENTS

This work is financially supported by the NSFC (11574161, 11674181, 11174182, 91750204, 61475077, and 11734009), the 111 Project (B07013), Program for Changjiang Scholars and Innovative Research Team in University (IRT_13R29), and the Fundamental Research Funds for the Central Universities.

[1] K. J. Vahala, Optical microcavities, Nature (London) **424**, 839 (2003).

[2] P. Del'Haye, A. Schliesser, O. Arcizet, T. Wilken, R. Holzwarth, and T. J. Kippenberg, Optical frequency comb generation from a monolithic microresonator, Nature (London) **450**, 1214 (2007).

[3] T. J. Kippenberg and K. J. Vahala, Cavity opto-mechanics, Opt. Express **15**, 17172 (2007).

[4] M. C. Collodo, F. Sedlmeir, B. Sprenger, S. Svitlov, L. J. Wang, and H. G. L. Schwefel, Sub-kHz lasing of a CaF_2 whispering gallery mode resonator stabilized fiber ring laser, Opt. Express **22**, 19277 (2014).

[5] J. Zhu, S. K. Ozdemir, Y.-F. Xiao, L. Li, L. He, D.-R. Chen, and L. Yang, On-chip single nanoparticle detection and sizing by mode splitting in an ultrahigh-Q microresonator, Nat. Photon. **4**, 46 (2010).

[6] S. M. Spillane, T. J. Kippenberg, O. J. Painter, and K. J. Vahala, Ideality in a Fiber-Taper-Coupled Microresonator System for Application to Cavity Quantum Electrodynamics, Phys. Rev. Lett. **91**, 043902 (2003).

[7] M. Cai, G. Hunziker, and K. Vahala, Fiber-optic add-drop device based on a silica microsphere-whispering gallery mode system, IEEE Photon. Technol. Lett. **11**, 686 (1999).

[8] M. Cai, P. O. Hedekvist, A. Bhardwaj, and K. Vahala, 5-Gbit/s BER performance on an all fiber-optic add/drop device based on a taper-resonator-taper structure, IEEE Photon. Technol. Lett. **12**, 1177 (2000).

[9] F. Monifi, J. Friedlein, S. K. Özdemir, and L. Yang, A robust and tunable add-drop filter using whispering gallery mode microtoroid resonator, J. Lightw. Technol. **30**, 3306 (2012).

[10] Q. Cao, H. Wang, C. Dong, H. Jing, R. Liu, X. Chen, L. Ge, Q. Gong, and Y. Xiao, Experimental Demonstration of Spontaneous Chirality in a Nonlinear Microresonator, Phys. Rev. Lett. **118**, 033901 (2017).

[11] P. F. Wang, M. Ding, G. S. Murugan, L. Bo, C. Y. Guan, Y. Semenova, Q. Wu, G. Farrell, and G. Brambilla, Packaged, high-Q, microsphere-resonator-based add-drop filter, Opt. Lett. **39**, 5208 (2014).

[12] P. Wang, M. Ding, T. Lee, G. S. Murugan, L. Bo, Y. Semenova, Q. Wu, D. Hewak, G. Brambilla, and G. Farrell, Packaged chalcogenide microsphere resonator with high Q-factor, Appl. Phys. Lett. **102**, 131110 (2013).

[13] M. Cai, O. Painter, and K. J. Vahala, Observation of Critical Coupling in a Fiber Taper to a Silica-Microsphere Whispering-Gallery Mode System, Phys. Rev. Lett. **85**, 74 (2000).

[14] M. L. Gorodetsky, A. A. Savchenkov, and V. S. Ilchenko, Ultimate Q of optical microsphere resonators, Opt. Lett. **21**, 453 (1996).

[15] L. Huang, J. Wang, W. Peng, W. Zhang, F. Bo, X. Yu, F. Gao, P. Chang, X. Song, G. Zhang, and J. Xu, Mode conversion in a tapered fiber via a whispering gallery mode resonator and its application as add/drop filter, Opt. Lett. **41**, 638 (2016).

[16] K. Wei, W. Zhang, L. Huang, D. Mao, F. Gao, T. Mei, and J. Zhao, Generation of cylindrical vector beams and optical vortex by two acoustically induced fiber gratings with orthogonal vibration directions, Opt. Express **25**, 2733 (2017).

[17] W. Zhang, K. Wei, D. Mao, H. Wang, F. Gao, L. Huang, T. Mei, and J. Zhao, Generation of femtosecond optical vortex pulse in fiber based on an acoustically induced fiber grating, Opt. Lett. **42**, 454 (2017).

[18] C.-L. Zou, Y. Yang, C.-H. Dong, Y.-F. Xiao, X.-W. Wu, Z.-F. Han, and G.-C. Guo, Taper-microsphere coupling with numerical calculation of coupled-mode theory, J. Opt. Soc. Am. B **25**, 1895 (2008).

[19] B. E. Little, J. P. Laine, and H. A. Haus, Analytic theory of coupling from tapered fibers and half-blocks into microsphere resonators, J. Lightw. Technol. **17**, 704 (1999).

[20] M. C. Frawley, A. Petcu-Colan, V. G. Truong, and S. N. Chormaic, Higher order mode propagation in an optical nanofiber, Opt. Commun. **285**, 4648 (2012).

[21] W. Zhang, L. Huang, F. Gao, F. Bo, L. Xuan, G. Zhang, and J. Xu, Tunable add/drop channel coupler based on an acousto-optic tunable filter and a tapered fiber, Opt. Lett. **37**, 1241 (2012).

Correction: The previously published Figure 3(b) contained an error and has been replaced.